ECE 445 FINAL PRESENTATION TEAM 10: NEUROBAND

By

Arrhan Bhatia

Vansh Rana

Vishal Moorjani

Final Report for ECE 445, Senior Design, Fall 2025

TA: Wenjing Song

9 December 2025

Project No. 10

Abstract

NeuroBand is a wearable human-computer interface designed to emulate a standard Bluetooth HID mouse for augmented reality applications. The system utilizes a distributed architecture consisting of a wrist subsystem with a mounted Inertial Measurement Unit (BNO086) for cursor tracking and a forearm subsystem with an electromyography (EMG) unit for gesture recognition. We have an ESP32 microcontroller (MCU) for each subsystem. These MCUs process sensor data, mapping wrist orientation to cursor coordinates and muscle activation to click events. The cursor tracking subsystem successfully demonstrated precise 2D navigation, battery life exceeds 4 hours with recharging circuitry and the EMG signals are processed using a machine learning model on the MCU to detect clicks and send via bluetooth to the user's host device.

Contents

1. Introduction

1.1 Purpose

As augmented reality (AR) glasses become more capable and integrated into daily life, a significant challenge remains in how users efficiently interact with them. Current input methods suffer from distinct limitations: voice commands are impractical in noisy public spaces and raise privacy concerns, camera-based hand tracking requires specific lighting conditions and an unobstructed line of sight, and gaze tracking often lacks the precision required for complex interfaces while causing eye strain over extended sessions.

To address these limitations, we developed NeuroBand, a wearable mouse controller designed for AR systems and PCs. The system creates a "Virtual Trackpad" on the user's arm by splitting functionality into two discreet wearable units. A wrist band maps wrist orientation to cursor movement on a 2D plane using an Inertial Measurement Unit (IMU), while a forearm band uses Electromyography (EMG) sensors to detect subtle muscle activations for "click" and "drag" gestures. The system emulates a standard Bluetooth Human Interface Device (HID) mouse, ensuring universal compatibility without custom drivers.

1.2 System Overview and Block Diagram

The NeuroBand system is divided into two primary subsystems: the Wrist Subsystem and the Forearm Subsystem.

The Wrist Subsystem serves as the central controller. It houses the primary microcontroller (ESP32-S3), which manages the Bluetooth Low Energy (BLE) link to the host device. It continuously reads orientation data from a BNO086 IMU to calculate relative cursor movement.

The Forearm Subsystem acts as a dedicated gesture engine. It utilizes an Analog Front End (ADS1298) to acquire differential EMG signals from the user’s forearm. A secondary microcontroller (ESP32-S3) processes these signals to detect gestures. When a "click" gesture is detected, the Forearm Subsystem transmits a digital signal to the Wrist Subsystem, which then packages the motion and click data into a single HID report for the host device.

Both subsystems are powered independently by Li-Ion batteries with dedicated power management circuits to ensure isolation and safety.

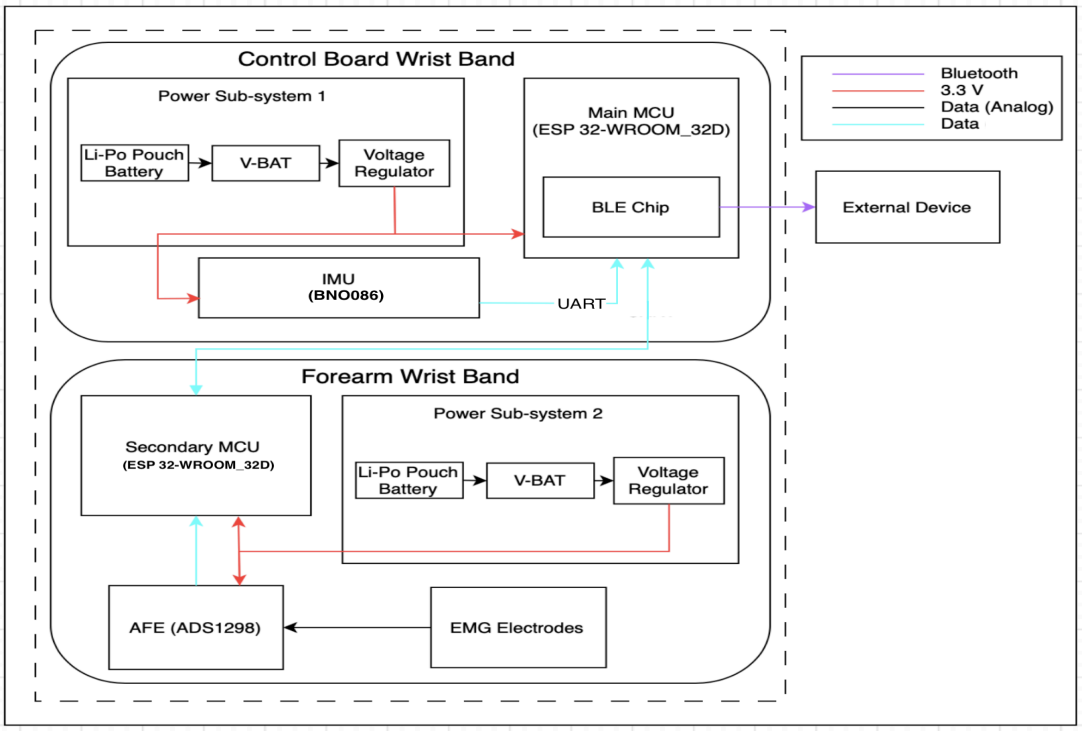

Figure 1: High Level Block Diagram

1.3 High Level Requirements

To function effectively as a daily driver for AR interaction, the system must meet the following performance metrics:

Responsiveness: The system must translate physical movement to cursor response with no perceptible lag. Specifically, the total latency from motion to cursor update must be less than 60 ms.

Gesture Accuracy: The EMG-based classification system must achieve at least a 90% true-positive rate for identifying click gestures to ensure a frustration-free user experience.

Battery Life: The combined system must operate continuously for a minimum of 4 hours on a single charge to support typical usage sessions.

1.4 Report Organization

This report details the engineering process behind NeuroBand. Chapter 2 outlines the design procedure, detailed component selection, and verification results for the wrist, forearm, and power subsystems. Chapter 3 provides a cost analysis and labor breakdown. Chapter 4 concludes the report by summarizing our accomplishments, analyzing the challenges faced regarding the machine learning model and discussing ethical considerations and future work.

1.5 Summary of Results

Our final verification confirmed that the power regulation and Bluetooth communication subsystems met all design specifications, with the device successfully pairing as a standard mouse and operating for over four hours on a single charge. The IMU-based pointer control provided smooth, responsive cursor movement. However, the EMG-based gesture recognition did not meet the targeted 90% accuracy rate due to difficulties in signal processing and model generalization.

2 Design

2.1 Wrist Subsystem

The Wrist Band serves as the central processing unit for the NeuroBand system. It is responsible for three critical functions: maintaining the Bluetooth Low Energy (BLE) Human Interface Device (HID) link with the host computer, acquiring and processing inertial data for cursor control, and fusing click events received from the Forearm Band.

2.1.1 Design Procedure

To achieve a "virtual trackpad" experience, we required a microcontroller capable of high-speed processing and robust wireless communication. We selected the ESP32-S3-WROOM-1 for the main MCU due to its integrated 2.4 GHz Wi-Fi and Bluetooth 5 capabilities, dual-core Xtensa LX7 processor, and ample peripheral interfaces (UART/I2C) required for sensor communication.

For the pointing mechanism, drift is a significant challenge in IMU-based input devices. Standard accelerometers and gyroscopes often suffer from accumulated error, making precise cursor control difficult. To mitigate this, we chose the BNO086 Inertial Measurement Unit (IMU). The BNO086 utilizes proprietary sensor fusion algorithms designed for virtual reality (VR) controllers, providing stable, drift-corrected quaternion data directly on-chip, which significantly offloads processing requirements from the main MCU.

2.1.2 Design Details

The Wrist Band PCB integrates the ESP32-S3 and BNO086, powered by a regulated 3.3 V rail. The BNO086 is configured to communicate with the MCU via a high-speed UART interface. To ensure ease of development and field updates, we incorporated auto-programming circuitry using MMBT3904 transistors on the DTR/RTS lines, allowing seamless code flashing via USB. Headers were also included to receive digital trigger signals from the Forearm Band. Figure 2 and figure 3 outline the schematics for the wrist band.

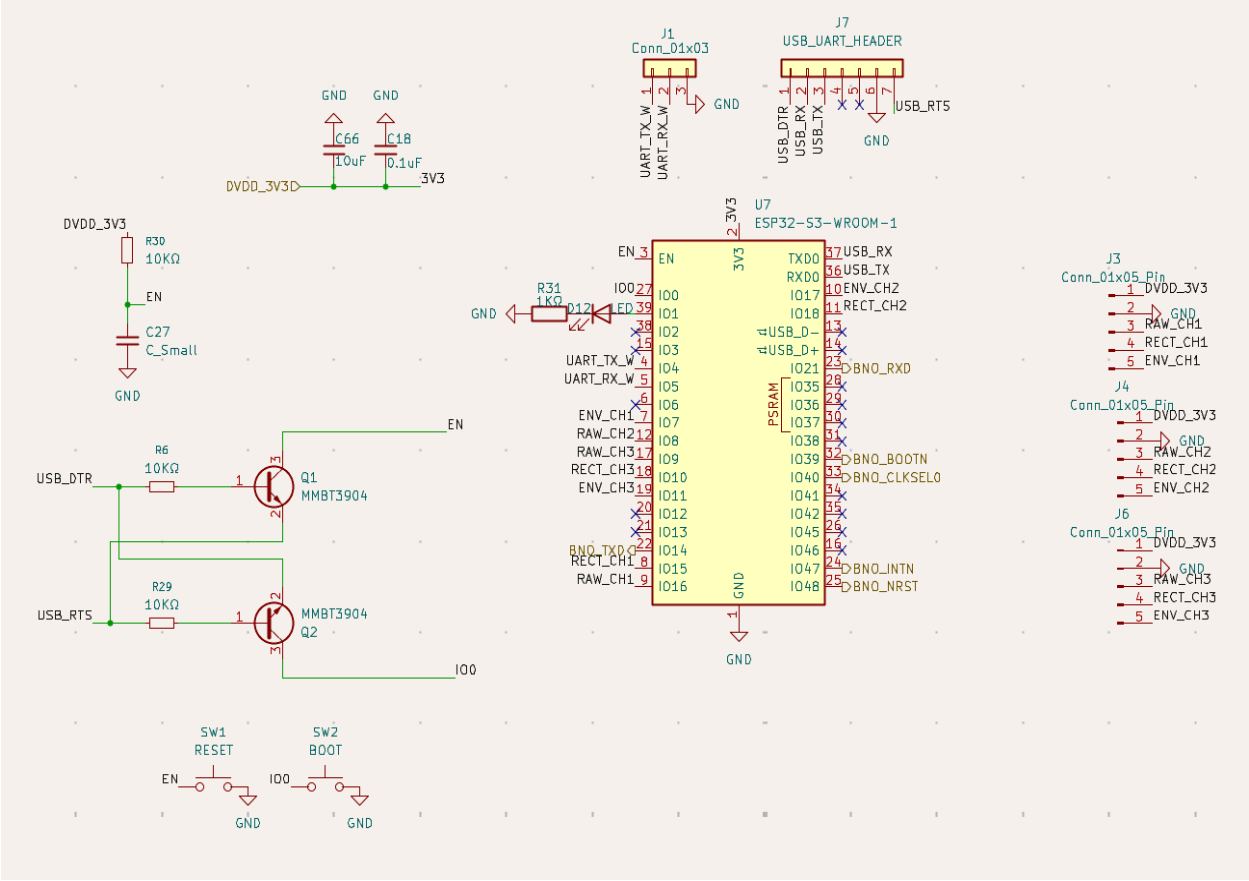

Figure 2: Wrist Band MCU schematic

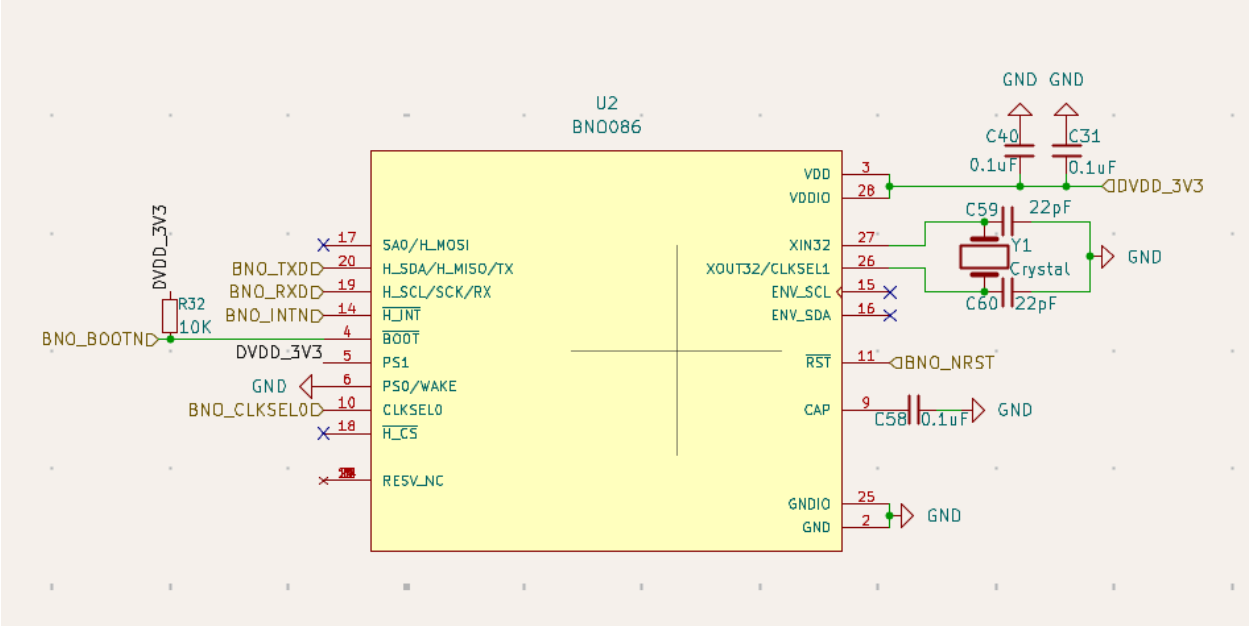

Figure 3: Wrist Band IMU schematic

Motion Processing Pipeline:

The firmware implements a specific motion pipeline to translate physical wrist movement into 2D cursor coordinates as seen in figure 4 below.

1. Data Acquisition: The ESP32 reads raw rotation vectors (quaternions) from the BNO086.
2. Conversion: The quaternions are converted into Euler angles (Yaw, Pitch, and Roll) to map the wrist's orientation in 3D space.
3. Differential Tracking: To prevent the cursor from jumping when the user's arm is in a comfortable resting position, we implemented a differential tracking algorithm. Instead of mapping absolute angles to absolute screen coordinates, the system calculates the change in angle between sampling frames.
    - dx=K* Delta(Roll)
    - dy=K*Delta(Pitch)
    - Where K is a sensitivity constant.
4. HID Reporting: These calculated deltas (dx,dy) are packetized into a standard BLE HID mouse report and transmitted to the host device.

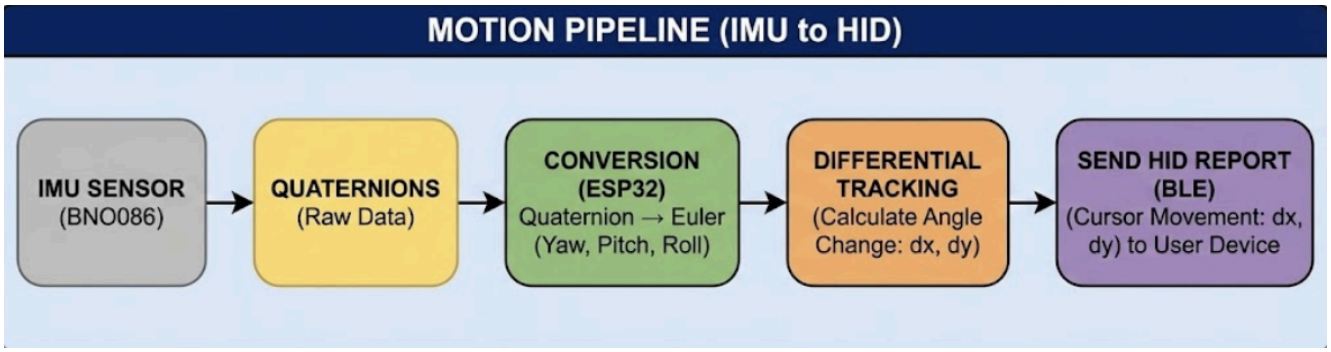

Figure 4: Motion Processing Pipeline on wrist subsystem

Clicking Pipeline:

The click generation process functions as a multi-stage relay system that bridges the separate Forearm and Wrist subsystems, as illustrated in figure 5 below. The process follows a linear four-step sequence:

1. Click Detection (Forearm): The pipeline initiates on the Forearm Board, where the ESP32 processes EMG signals to detect a muscle contraction (squeeze) event.
2. Signal Transmission: Upon validating a click, the Forearm Board drives a dedicated GPIO output pin High, sending a digital '1' signal across the wired interface connecting the two bands.
3. Signal Reception: The Wrist Board MCU (ESP32) continuously monitors its corresponding digital input pin. It detects the rising edge of the incoming digital '1' signal from the forearm unit.
4. HID Event Dispatch: Immediately upon detecting the signal, the Wrist MCU maps the input to a standard "Left Click" mouse event. This event is then packetized into the Bluetooth Low Energy (BLE) report and transmitted to the user device, successfully emulating a hardware mouse click.

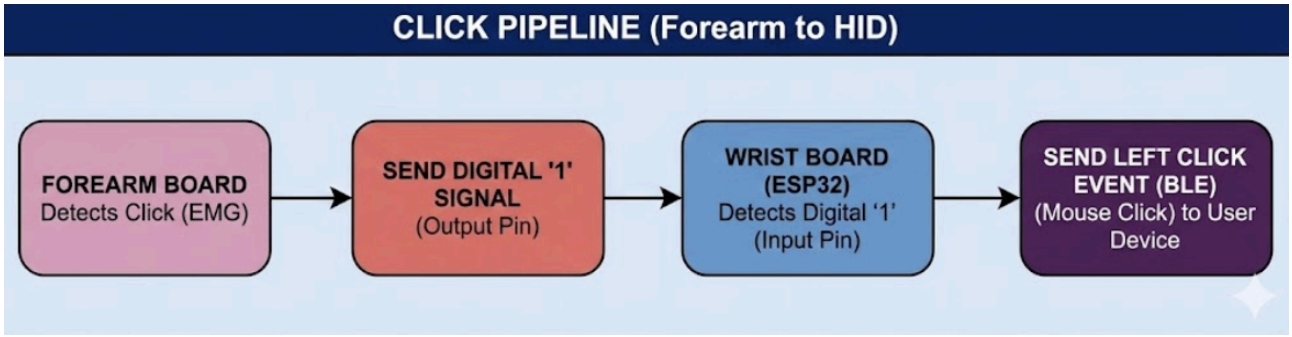

Figure 5: Click Pipeline on wrist subsystem

2.1.3 Design Verification

We verified the wrist subsystem against the high-level requirements defined in the design phase.

1. Bluetooth Connectivity: The device was powered on and set to broadcast BLE advertisements. We successfully paired it with a MacBook Pro, where it was immediately recognized as a "ESP32 Wrist Mouse" without requiring custom drivers. Verification for this can be seen in figure 6 below.

2. Cursor Latency and Smoothness: We tested latency by rotating the PCB along the X (Roll) and Y (Pitch) axes and observing the cursor response on the host screen. The requirement was for the system to translate physical movement to cursor movement with no perceptible lag (> 0.5s). Visual inspection confirmed immediate response times, with smooth travel and no significant jitter.

3. Battery Life: Current draw was measured during normal operation (continuous IMU polling and BLE transmission). The average power consumption was verified to be within limits that support the >= 4 hour battery life requirement using the selected 1100 mAh Li-Ion battery.

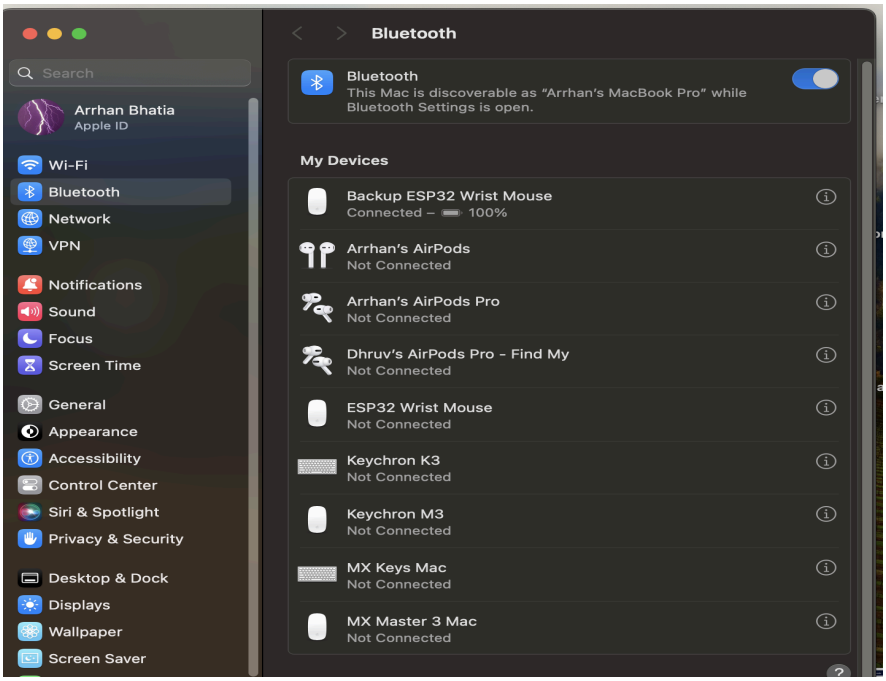

Figure 6: Click Pipeline on wrist subsystem

2.2 Forearm Subsystem

The Forearm Band acts as a dedicated gesture engine. Its primary function is to process noisy biological signals in real-time to distinguish between a "Rest" state and a "Squeeze" (Click) state. It is responsible for reading, filtering, and processing the data without any noticeable latency.

2.2.1 Design Procedure

Electromyography (EMG) signals are inherently low-amplitude (microvolts) and susceptible to power line interference (60 Hz) and motion artifacts. To ensure reliable signal acquisition, we separated the analog acquisition from the main digital communications board. We selected the ADS1298 Analog Front End (AFE) because of its high precision, simultaneous sampling capabilities, and integrated Right Leg Drive (RLD) pin, which is essential for biasing the body and rejecting common-mode noise.

For processing, we utilized a secondary ESP32-S3-WROOM-1. While the Design Document initially proposed an STM32, the ESP32-S3 was chosen for the final implementation due to its vector instructions which accelerate neural network inference, allowing us to run the gesture classification model directly at the "edge". To develop the model, we knew that we would need a model architecture that would look at patterns along with the raw values. So, we chose a 1D CNN architecture. To balance performance and latency when deployed on the ESP-32, we developed a 3 Layer CNN. We also experimented with oversampling squeezed values, shifting labels back to account for delay between activation and the fingers actually making contact, and deadzoning uncertain regions. The results of these experiments are covered in Figure 9 below.

2.2.2 Design Details

The hardware pipeline consists of three differential EMG channels connected to the ADS1298. The AFE is configured with a gain of 6x and a sample rate of 500 Samples Per Second (SPS). The internal RLD amplifier is connected to a reference electrode to actively cancel 60 Hz mains hum.

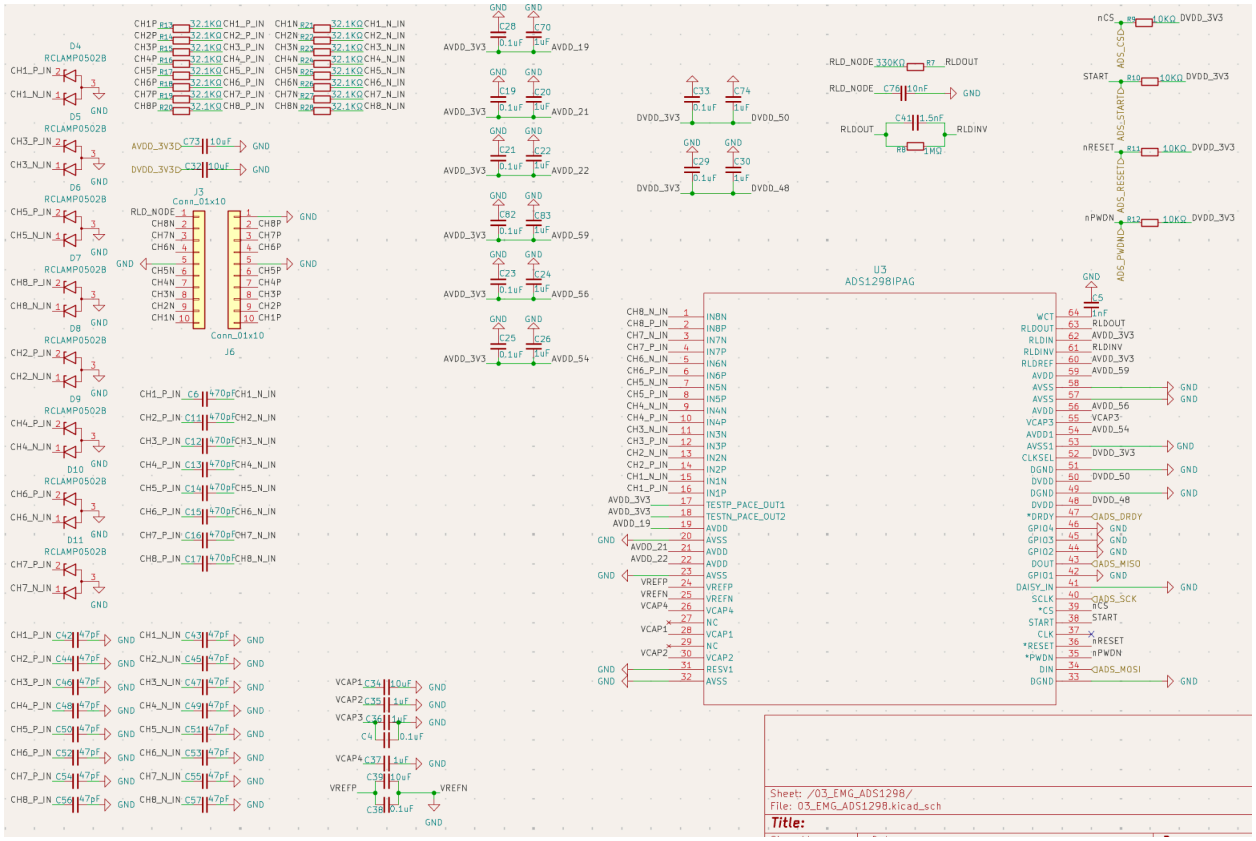

Figure 7: Forearm MCU schematic

Digital Signal Processing (DSP) Raw data from the AFE is processed by the ESP32-S3 through a three-stage software pipeline :

1. **Buffering:** A 300 ms rolling window buffer captures transient muscle spikes.
2. **Bandpass Filtering:** A 4th-order Butterworth filter (20–150 Hz) removes low-frequency motion artifacts and high-frequency noise.
3. **Notch Filtering:** A digital 60 Hz notch filter further suppresses power line interference.

Machine Learning Classifier The filtered data is fed into a 1D Convolutional Neural Network (CNN) designed for temporal pattern recognition. The model architecture consists of:

- **Input Layer:** (150 time steps, 3 channels).
- **Feature Extraction:** Three blocks of Conv1D layers (16, 32, and 64 filters) with Batch Normalization and ReLU activation to extract temporal features from the muscle signals.
- **Downsampling:** MaxPooling1D layers reduce dimensionality.

- **Classification:** A Global Average Pooling layer feeds into a Dense layer (32 units) and a final Sigmoid output unit to classify the signal as binary "Click" or "No Click".

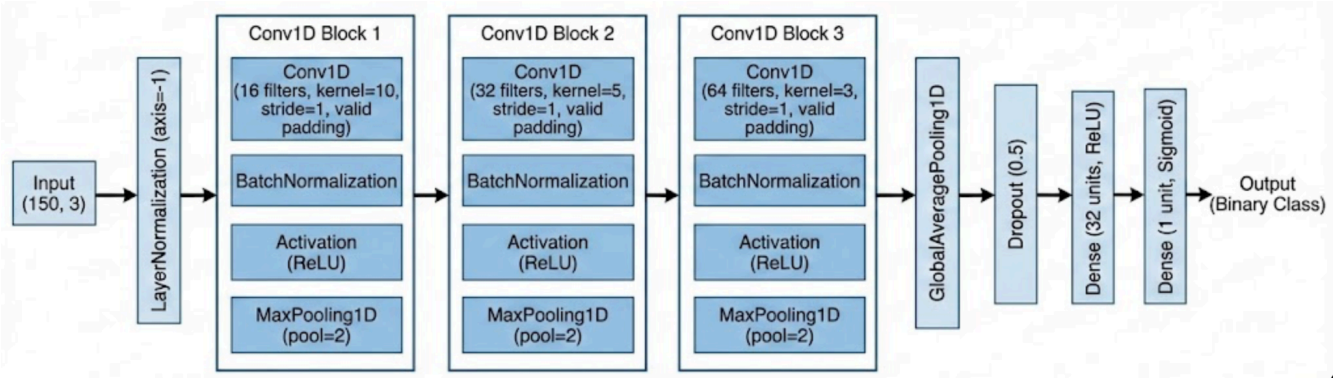

Figure 8: Machine Learning model architecture

2.2.3 Design Verification

We verified the Forearm Subsystem against the requirements for the scope of this subsystem. Some of our verification results can be seen in figure 9 below:

1. Battery Longevity: We measured current draw during continuous inference mode. The system achieved the >=4-hour battery life requirement, validating the power budget calculations .

2. Machine Learning Performance: The verification goal was a >90 true positive rate for click detection. We trained and tested the model across 95 different configurations.

- **Quantitative Analysis:** The median F1 score across configurations was only 0.009, with the best configuration achieving an F1 score of 0.564 . While the system could detect muscle activity, it struggled to generalize across different arm positions and electrode placements, leading to a high rate of false negatives and erratic behavior .

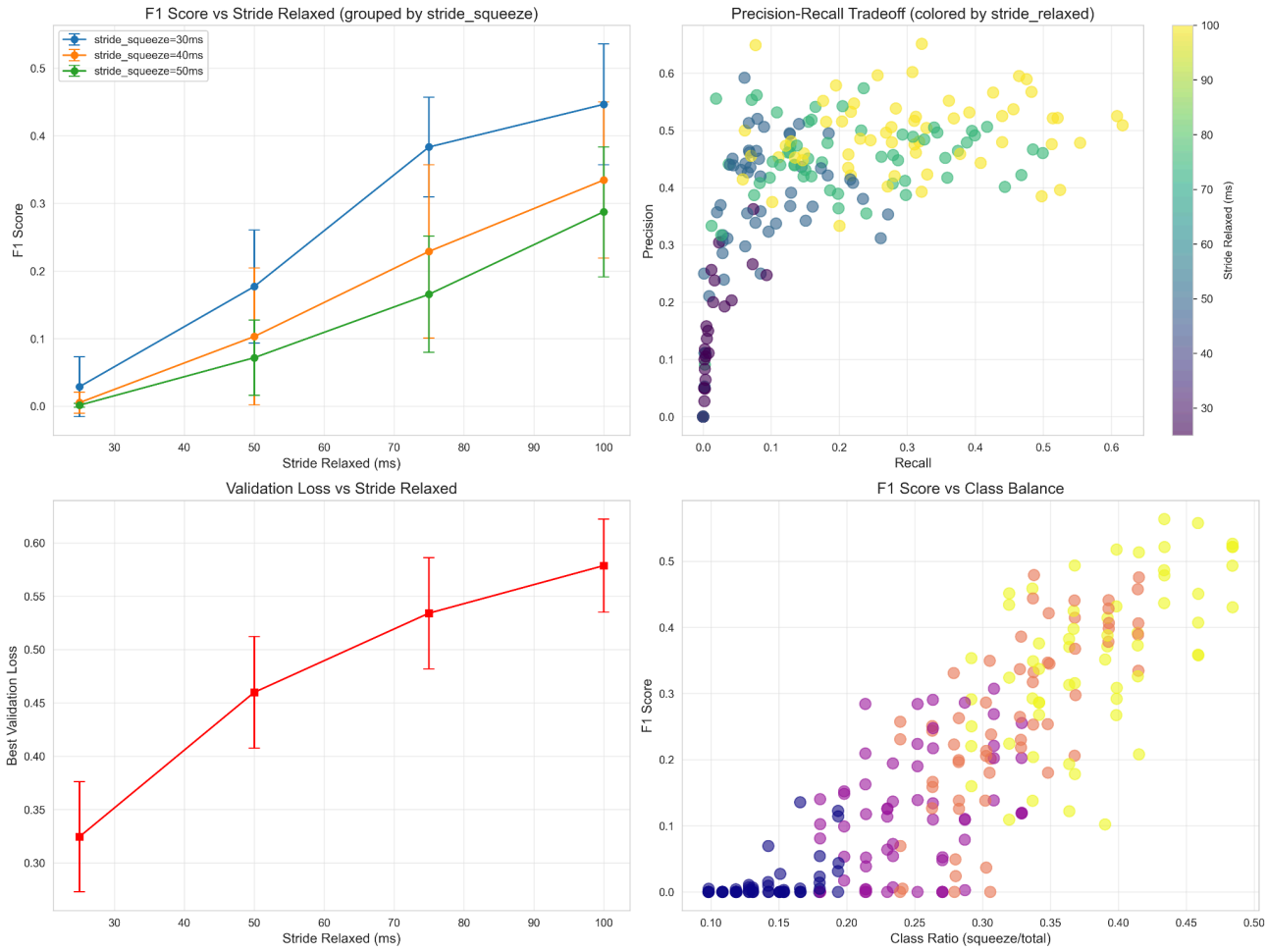

Figure 9: Forearm machine learning model verification results

2.3 Power Subsystem

To ensure user safety and signal integrity, we implemented a Split-Power Topology where the Wrist and Forearm bands operate on completely independent power domains. This design choice provides two key benefits: it eliminates the need for running power cables along the user's arm, reducing weight and snag hazards, and it isolates the sensitive analog EMG circuitry from digital switching noise.

2.3.1 Design Procedure

Safety was the primary constraint for the power system since the device is worn directly on the skin. We selected 3.7 V Li-Ion batteries for their high energy density and slim form factor. For voltage regulation, a standard buck-boost IC was sufficient for the digital components (MCUs), but the EMG Analog Front End required a cleaner supply. Therefore, we have a ferrite bead to separate the analog and digital rails. To future proof the design and make using it convenient we added in USB-C charging with circuitry to regulate the maximum charging and discharging current to prevent overheating.

2.3.2 Design Details

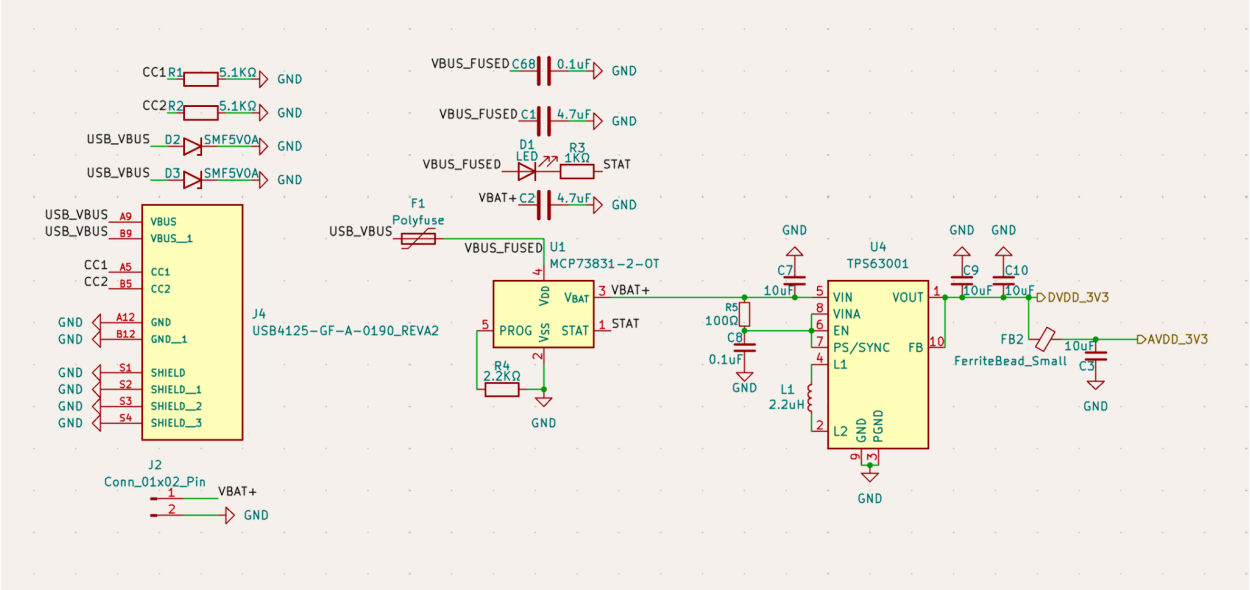

Figure 10: Power subsystem schematic

We use a 6 pin USB-C receptacle that is set in sink mode (will only receive power) using the CC resistors. We have also added TVS Diodes to protect the PCB from any transient voltage spikes. We use a polyfuse to protect the circuit from any surges in current. To regulate the charging and discharging current we use the MCP73831 IC, and to set the current we use the Rprog resistor. Since we would like to regulate the current to 425mA (<0.5 C rate for 1100mAH Li-Ion battery), we set the value of Rprog to 2.2KΩ. We also added in a charging status LED on the STAT pin. The battery also gets connected to the TSP63001 buck-boost converter, which regulates the voltage to 3.3V to power the MCU, AFE, and IMU. The analog rail that powers the analog components is separated from the digital rail using a ferrite bead to ensure as little noise on the AFE power lines as possible.

2.3.3 Design Verification

We tested the power subsystem to ensure that all components are powered by voltages within their supported ranges, and they receive sufficient current. To meet the requirements of the components, as well as to ensure safety of the user, we verified the following:

1. Input voltage is regulated to 3.3V for all components: Using an oscilloscope we measured the voltage at the input pin of the MCU, the ADS1298, and the IMU to ensure that all components receive a stable 3.3V during operation. We tested the input voltage during all stages of operation.
2. Maximum Charging Current is 425 mA: Using a multimeter we calculated the current draw in series. We charged the battery from 0%-100% and ensured that the charging current did not exceed 425mA. We also measured the current during discharging to ensure that it fell in the standard range for operation.

3. Costs

3.1 Parts

Table 1: List of Parts

Part	Manufacturer	Retail Cost ($) / unit	Bulk Cost ($) / unit	Actual Cost ($)
0.1uF Capacitor	Kemet	0.08	0.01	1.68
1.5nF Capacitor	Vishay	1.45	0.53	1.45
100Ω Resistor	Yageo	0.10	0.01	0.20
10KΩ Resistor	Bourns Inc.	0.10	0.00	1.10
10nF Capacitor	Kemet	0.24	0.05	0.24
10uF Capacitor	Kyocera Avx	0.42	0.11	5.46
1KΩ Resistor	Bourns Inc.	0.10	0.00	0.40
1MΩ Resistor	Bourns Inc.	0.10	0.00	0.10
1nF Capacitor	Kyocera Avx	0.29	0.11	0.29
1uF Capacitor	Kemet	0.27	0.10	2.92
2.2KΩ Resistor	Bourns Inc.	0.03	0.00	0.05
2.2uH Inductor	Coilcraft	1.46	0.68	2.92
22pF Capacitor	Samsung Electro-Mechanics	0.04	0.01	0.08
32.1KΩ Resistor	Panasonic Electronic Components	0.06	0.04	0.92
330KΩ Resistor	Bourns Inc.	0.03	0.01	0.03
4.7uF Capacitor	Taiyo Yuden	0.24	0.10	0.94
470pF Capacitor	Yageo	0.06	0.02	0.44

47pF Capacitor	Yageo	0.05	0.01	0.77
5.1K Resistor	Bourns Inc.	0.03	0.00	0.10
ADS1298	Texas Instruments	45.86	32.87	45.86
BNO086	Ceva Technologies Inc.	13.40	9.05	13.40
Tactile Switch	Omron Electronics Inc.	0.60	0.52	2.40
Battery Header	JST Sales America Inc	0.10	0.05	0.20
Headers	JST Sales America Inc	1.00	0.59	4.00
Crystal	TXC Corporation	0.68	0.42	0.68
ESP32-S3-WROOM1	Espressiff Systems	6.56	4.21	13.12
Ferrite Bead	Murata	0.10	0.02	0.10
LED	Bivar	0.48	0.21	1.90
MCP73831	Microchip Technology	0.76	0.58	1.52
MMBT3904 Transistor	Diotec	0.06	0.01	0.26
Polyfuse	Littelfuse Inc.	0.47	0.19	0.94
TVS Diode Pair	Semtec Corporation	0.79	0.36	6.30
TVS Diode Single	Vishay	0.12	0.10	0.47
Buck Boost Converter	Texas Instruments	1.81	1.24	3.62
USB C Receptacle	GCT	0.51	0.32	1.01
Li-Ion Battery	EEMB	5.63	-	11.26
Electrodes	3M	0.30	0.30	2.10
Total				129.23

3.2 Labor

The average computer engineering major from UIUC makes ~$118,000. For a 40 hour work week, that comes out to ~$57 hourly. Each of us has spent ~25 hours per week on this assignment, which works out to ~$171,000 in labor costs.

4. Conclusion

4.1 Accomplishments

We successfully designed and fabricated a functional wearable interface that partially realizes the "virtual trackpad" concept. The power subsystem was fully verified, providing a stable 3.3 V rail and safely charging the Li-Ion batteries with a regulated 425 mA current, ensuring a runtime exceeding four hours. The Wrist Band subsystem successfully established a low-latency Bluetooth Low Energy (BLE) link with a host device, recognized immediately as a standard HID mouse without custom drivers . The IMU-based motion pipeline demonstrated high-fidelity cursor control, translating physical wrist rotation into smooth 2D pointer movement on the screen with no perceptible latency . The system integration proved that a distributed architecture using separate MCUs for sensing and communication is viable for wearable form factors .

4.2 Uncertainties

The primary uncertainty in our final design lies in the Forearm Band's gesture recognition capabilities. While the hardware successfully captured EMG signals, the Machine Learning classifier failed to meet the verification requirement of a >90% true positive rate.

Quantitative analysis of the model showed a median F1 score of only 0.009 across 95 tested configurations, with the best-performing configuration achieving only 0.564 . This shows that the model is certainly learning some patterns, but the low score is attributed to two main factors:

1. **Signal Variability:** The rigid PCB design made it difficult to maintain consistent electrode contact with the skin, leading to significant noise and motion artifacts that the software filters could not fully remove. Further, without having snap connectors for the electrodes we had significant movement of the cables even during operation.
2. **Model Generalization:** The 1D CNN model struggled to generalize across different arm positions, resulting in a high false-negative rate where valid muscle squeezes were often ignored. Since we struggled with an imbalance dataset, we had to oversample squeeze samples by using a smaller stride across them than the rest values. From figure 9 we clearly see that this boosts model performance. So, having a better dataset and a deeper model will likely result in significantly improved performance.

4.3 Ethical considerations

We ground our work in the **IEEE and ACM Codes of Ethics**, prioritizing user safety and public interest .

- **Safety:** Because the device sits directly on the skin, safety was a primary design constraint. We utilized low-voltage 3.7 V Li-Ion cells with integrated protection and a dedicated charge controller to prevent thermal runaway . All exposed conductive parts were insulated, with the exception of the EMG electrodes intended for bio-potential sensing .

- **Honesty:** We present NeuroBand strictly as a human-computer interface and not a medical diagnostic product . We have transparently reported the limitations of our gesture recognition system rather than exaggerating its capabilities.
- **Privacy:** The device treats motion and EMG signals as sensitive data. Inference occurs entirely on the edge (on the ESP32), and no raw biological data is stored or transmitted to the cloud, ensuring user privacy .

4.4 Future work

To address the uncertainties and improve the device for a production-ready standard, we propose the following upgrades:

- **Flexible PCBs:** The current rigid boards were bulky and uncomfortable. Switching to flexible PCBs would allow the circuit to conform to the curvature of the arm, drastically improving ergonomics and ensuring consistent electrode contact for better signal quality .
- **Unified Architecture:** We would consolidate the Forearm and Wrist PCBs into a single flexible unit. This would simplify the power architecture to a single battery and eliminate the wired UART link, reducing weight and failure points .
- **Advanced Gestures:** By utilizing all 8 analog channels of the ADS1298 (currently only 3 are used), we could train a more robust model to support complex interactions like scrolling, zooming, or rotating .
- **Haptic Feedback:** Integrating Linear Resonant Actuators (LRA) would provide tactile confirmation of clicks, significantly improving the user experience .

References

"ADS1298 Data Sheet, Product Information and Support | TI.com." *Www.ti.com*, www.ti.com/product/ADS1298.

Association for Computing Machinery. "ACM Code of Ethics and Professional Conduct." *Association for Computing Machinery*, 22 June 2018, www.acm.org/code-of-ethics.

BNO08X Datasheet Revision 1.16 BNO08X Data Sheet.

"DigiKey Electronics - Electronic Components Distributor." *Www.digikey.com*, www.digikey.com.

"Espressif Documentation." *Espressif.com*, 2025, documentation.espressif.com/esp32-s3_technical_reference_manual_en.pdf.

IEEE. "IEEE Code of Ethics | IEEE." *Ieee.org*, 2020, www.ieee.org/about/corporate/governance/p7-8.

MCP73831/2 Features.

"Mouser Electronics." *Mouser.com*, 2024, www.mouser.com.

Appendix A Requirement and Verification Table

Table 2: System Requirements and Verifications

Subsystem	Requirement	Verification Methodology	Results
ESP32 MCU + IMU (Wrist subsystem)	The subsystem broadcasts BLE advertisements and successfully pairs with a host computer	Power on PCB, open the bluetooth settings on laptop and verify that device connects as mouse.	Pass
	The subsystem must translate physical movement to cursor movement with perceptible real-time response (no visible lag > 0.5s).	Ensure the device is connected via Bluetooth. Rotate the PCB along the X-axis (Roll) and verify the cursor moves Left/Right. Tilt the PCB along the Y-axis (Pitch) and verify the cursor moves Up/Down.	Pass
	The ESP32 must successfully initialize communication with the BNO086 IMU over the UART interface.	Connect ESP32 to a laptop via USB and open the Arduino Serial Monitor (115200 baud). Verify that the message "BNO086 found!" appears in the log when powering up. confirming the handshake is successful.	Pass
	>=4H Battery Life	Measure current draw during Normal Operation, and mathematically verify operation time of battery.	Pass
ESP32 MCU + ML Model (Forearm subsystem)	>90% true positive rate for clicking on ML model	Measure model performance on a validation set to ensure accuracy requirements are met	Fail
	>=4H Battery Life	Measure current draw during Normal Operation, and mathematically verify operation time of battery.	Pass
Power Subsystems	Output voltages regulated to 3.3 V	Use an oscilloscope to verify that output voltages from both buck-boost converters and voltage at the VCC of the MCU is at 3.3V during operation.	Pass
	Recharges at 425mA	Measure current using a multimeter in series between the charging chip output and simulated dead battery - a high wattage resistor.	Pass